High temperature nuclear cogeneration utilizing supercritical CO_2 for enhanced thermal efficiency

Babras Khan[a], Himani Anand Meshram[b], Vaclav Dostal[a,*]

[a]CTU in Prague, Department of Energy Engineering, Technicka 4, Prague, 160 00, Czech Republic

[b]Commonwealth Scientific and Industrial Research Organisation (CSIRO), Research Way Clayton, Vic 3168, Australia

[*]Corresponding author. E-mail: *khanbabr@cvut.cz*

ABSTRACT

This study addresses the challenge of clean energy production for industrial applications, emphasizing nuclear power role in meeting economic, security, and environmental sustainability goals. A thermodynamic analysis was conducted on a high-temperature nuclear reactor integrated with an sCO_2 Brayton cycle and a reboiler. The system performance was assessed by varying turbine inlet temperature and compressor pressure ratio. Results indicate that higher reboiler CO_2 inlet temperatures significantly enhance power cycle efficiency up to an optimal threshold. Enhancing turbine efficiency substantially improves thermal efficiency, whereas compressor efficiency has a less pronounced impact. Whereas, net power output increases with higher turbine inlet temperatures and compressor pressure ratio, peaking at 725°C and a pressure ratio of 4.0. These insights are vital for optimizing the design and operation of nuclear-driven thermal power systems to maximize efficiency and net power output.

Keywords: Nuclear; Supercritical CO_2; Brayton cycle, Thermal efficiency

1. Introduction

The global energy demand is steadily rising, while fossil fuel resources are being depleted, and the threat of climate change looms large. The combustion of fossil fuels generates greenhouse gases, which significantly harm the environment and are a primary driver of unpredictable global climate change [1]. To tackle these global energy and environmental challenges, it is essential to enhance the energy efficiency of our industries [2]. Thus, identifying alternative energy sources is essential to address this urgent global challenge. Researchers are exploring several viable options for energy generation, including solar energy [3], nuclear power [4], geothermal energy, flue gas from biogas combustion, and waste heat [5]. Utilizing clean energy, reducing pollutant emissions, and enhancing energy conversion efficiency are key strategies to combat the rising demand for fossil fuels and severe environmental pollution [6]. The supercritical carbon dioxide (sCO_2) is a promising solution, offering an eco-friendly, non-toxic, inexpensive, and inert working fluid [7]. This cycle achieves higher efficiency than conventional power cycles, particularly when used with medium- and high-temperature heat sources like waste heat, solar energy, and nuclear energy. Nuclear energy has seen rapid development recently due to its environmental friendliness, cost-effectiveness, and reliability. With the advancement of Generation IV nuclear reactors, the future of nuclear power generation looks promising [8].

Clean energy production is a top priority in Europe and is increasingly recognized as a global necessity. To date, most efforts have focused on electric power generation due to its relatively straightforward solutions. However, electricity represents only 18% of total energy consumption. Other sectors, such as heating and transportation, rely almost entirely on fossil fuels like natural gas, oil, and coal, which are major sources of high emissions [9]. In Europe, electricity constitutes 24% of energy consumption, while heating and cooling for residential and industrial purposes account for 50%. Nearly all of the heat derived in this sector comes from combustion. Therefore, an effective European energy policy must prioritize addressing this sector, even though it often goes unnoticed by the general public. The anticipated political and socio-economic benefits of such a policy are substantial [10]. The European Nuclear Cogeneration Industrial Initiative has conducted the GEMINI+ project with the aim of advancing the industrial demonstration of a High Temperature Gas-cooled Reactor (HTGR) power plant for cogeneration purposes [11].

The sCO_2 recompression cycle presents a more efficient, significantly simpler, and more compact alternative to the superheated steam cycle. Compared to the helium Brayton cycle, it is notably less complex. At 550°C, the sCO_2 recompression cycle achieves a thermal efficiency of 46%, matching the helium Brayton cycle's efficiency, which is only reached at 800°C [12]. To meet electrical power needs, an energy conversion system that matches its core power and temperature is crucial. Due to the high thermal efficiency and power output requirements, a dynamic power cycle system is preferred. With a core outlet temperature up to 700°C, the Rankine cycle is unsuitable because it lacks compactness and efficiency. Thus, the Brayton cycle system is chosen. The sCO_2 Brayton cycle is promising for its high thermal efficiency, compact design at turbine inlet temperatures of 500°C to 700°C, and reduced water consumption [13].

In the EU, 26% of industrial heat demand requires temperatures above 400°C, which is mainly met by burning fossil fuels [14]. In the UK, the iron and steel, mineral products, and food and drink sectors are the most energy-intensive, consuming over 50% of industrial process heat [15]. Industrial heat applications account for 14% of the UK's carbon dioxide emissions. High-temperature heat from nuclear power plants could potentially eliminate these emissions, but the use of nuclear energy for processing heat is still limited internationally [16]. Europe is currently facing major issues with material and energy resources that threaten industrial operations. Considering the advancements and benefits of small modular reactors (SMRs), [17]propose integrating SMRs into regions with industrial plants. The sCO_2 recompression cycle is ideal for nuclear reactors with core outlet temperatures above 500°C, in both direct and indirect versions. Additionally, it has the potential to reduce capital costs compared to Rankine steam or helium Brayton cycles [18].

European Commission report[19] summarizes the energy consumption breakdown in the EU27 for 2005 and 2009, as shown in the Table 1. The data for the first four columns is sourced from EURSTAT, while the useful heat demand is estimated in his report. The estimated useful heat consumption for the industry was 5,349 PJ in 2005 and 4,434 PJ in 2009. Fig. 1, presents the projected useful heat demand in the industrial sector. HTGR can address much of this demand. Development programs in the UK, Germany, and the US, along with R&D projects in Europe, China, Japan, South Korea, and other countries, have advanced HTGR technology to a relatively high Technology Readiness Level [20]. Currently, the primary market for processing heat relies on steam at around 550°C. However, there is a significant and expanding demand for bulk hydrogen, which holds substantial potential for further growth. This paper focuses on GEMINI+ studies investigating the utilization of process heat from a nuclear cogeneration sCO_2 Brayton cycle for various industrial applications, which are of interest to many industrialized countries.

Table 1. Break-down of energy consumption in European Industry.

PJ	Total Final energy	Total Final energy	Electrical energy	Electrical energy	Useful heat demand	Useful heat demand
Years	**2005**	**2009**	**2005**	**2009**	**2005**	**2009**
Iron and steel	2622	1853	488	393	1695	1147
Nonferrous metals	486	373	291	223	149	113
Chemicals	2480	2109	736	629	955	877
Nonmetallic minerals	1820	1529	298	267	1209	937
Paper and pulp	1476	1383	510	443	549	512
Food, drink and tobacco	1261	1149	401	393	481	418
Textiles	331	216	119	85	120	72
Other industries	3163	2669	1228	1099	191	358
Total	13640	11282	4072	3532	5349	4434

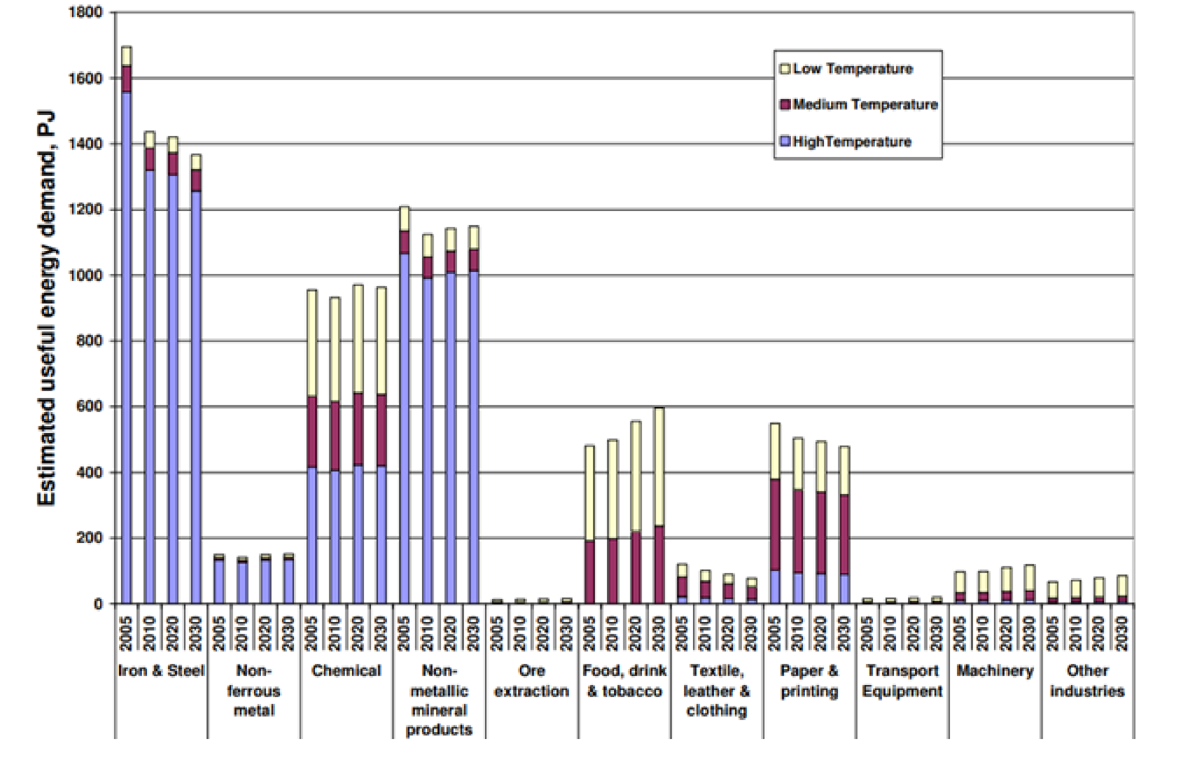

Fig. 1. Estimated useful heat demand in the European Industry.

2. sCO_2 Brayton cycle

2.1 sCO_2 as working fluid

Supercritical carbon dioxide (sCO_2) power cycles offer the potential for higher thermal efficiencies and lower capital costs compared to current steam-based power cycles. These distinctive attributes of sCO_2 are generating significant interest in its application for power generation [21]. Carbon dioxide reaches its critical pressure (7.3773 MPa) and critical temperature (304.12 K) at the critical point. As illustrated in Fig. 2, sCO_2 has a density similar to liquid but retains the viscosity and diffusion properties of a gas, exhibiting gas-like behavior with liquid density during expansion. It is non-toxic, non-corrosive, non-flammable, and non-explosive, with abundant availability and a reasonable price costing just 1/10th of helium and 1/70th of the organic working fluid R-134a. Therefore, recycling is unnecessary. Additionally, it is compatible with standard materials and lubricants and poses no environmental harm.

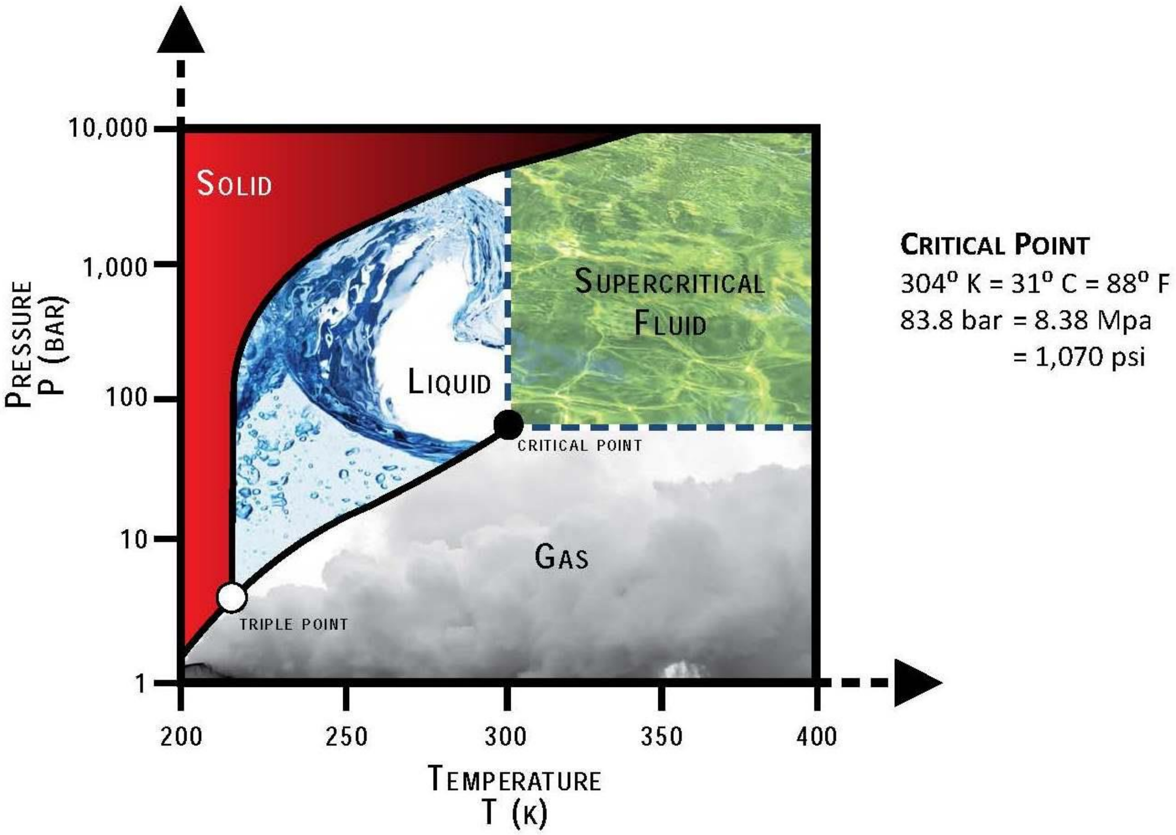

Fig. 2. Carbon dioxide pressure-temperature phase diagram.

Compared to other working fluids used in the supercritical Brayton cycle, carbon dioxide offers advantageous qualities such as a low critical point and high critical density. The physical properties of CO_2 are detailed in Table 2.

Table 2. Properties of selected working fluids for the supercritical Brayton cycle.

Fluids	CO_2	H_2O	He	Air
Molecular weight	44.01	18.015	4.0026	28.965
Critical density/kg.m−3	467.6	322	72.567	342.68
Critical temperature/K	304.13	647.1	5.1953	132.53
Critical pressure/MPa	7.3773	22.064	0.2276	3.786

3. System Description and Assumption

The schematic layout shown in Fig. 3 represents a nuclear cogeneration system integrated with the sCO_2 Brayton cycle, allowing for efficient power generation and heat utilization. The system consists of several key components and processes.

A nuclear reactor operates with a thermal power output of 180 MWth and uses helium (He) as a primary coolant. Before coolant leaves the reactor, it is heated to 750°C at a pressure of 6 MPa. It then transfers heat through a heat exchanger to a supercritical carbon dioxide working fluid, which is then cooled to 325°C. After the heat is exchanged, the pump circulates the cooled helium back into the reactor for reheating.

In the sCO_2 Brayton cycle, sCO_2 is first compressed to raise its pressure for the heat exchange process. This compressed sCO_2 is preheated by recovering heat from the turbine exhaust before it enters the primary heat exchanger, where it absorbs heat from the helium coolant, leading to an increase in both temperature and pressure. The high-temperature and high-pressure sCO_2 then expands through turbine, generating electricity. This mechanical energy is then converted into electrical energy by a generator, which powers the internal electrical needs of the nuclear plant. After expansion, sCO_2 passes through the recuperator to transfer some of its remaining heat to the incoming compressed sCO_2. It is then further cooled in the economizer before entering the cooler, where it is brought back to its initial state, completing the cycle. Additionally, the residual heat from the sCO_2 cycle is utilized in a reboiler to produce process steam at 540°C, with a mass flow rate of 64 kg/s and a pressure of 13.8 MPa. This steam is supplied to the end-user site for various industrial applications. The condensed steam at 200°C is returned from the end-user site to the reboiler for reheating.

The entire system is designed to optimize heat utilization from nuclear reactor, where the sCO_2 Brayton cycle is essential for power generation and heat recovery. The reboiler efficiently utilizes excess heat energy to generate industrial steam, thereby increasing the overall energy efficiency of the system. In summary, this integrated system combines a nuclear reactor with sCO_2 Brayton cycle and a reboiler, ensuring effective energy conversion and utilization, which enhances the efficiency of the system.

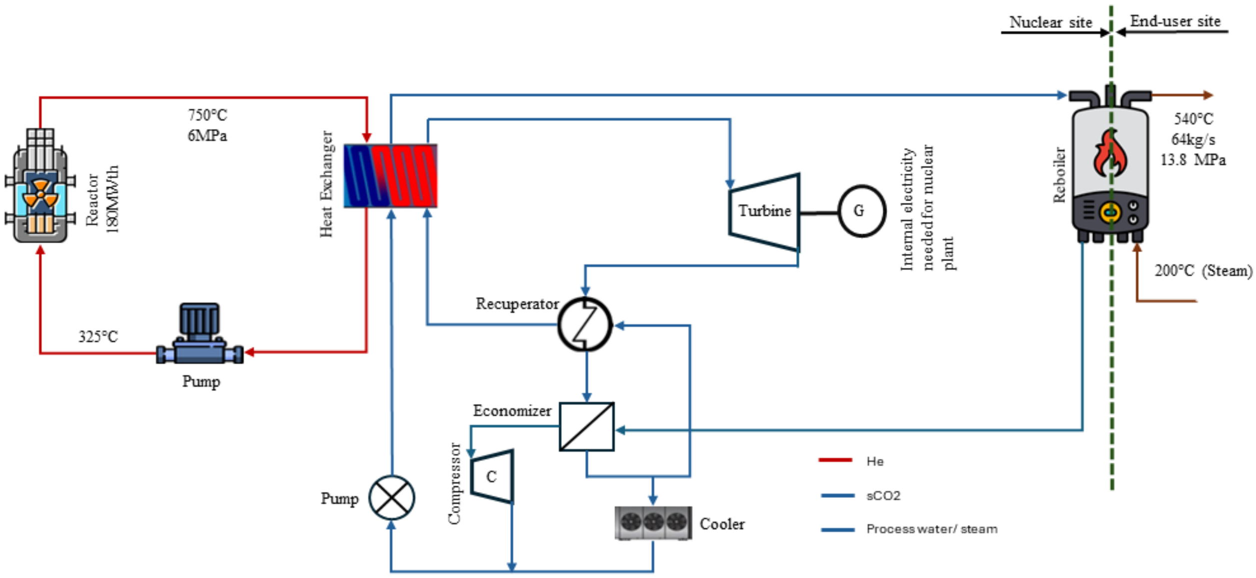

Fig. 3. Schematic layout of nuclear cogeneration with sCO_2 Brayton cycle.

The T-S diagram in Fig. 4 represents the temperature-entropy relationship at various state points in the cycle. The state points are plotted, and the saturation dome is included to provide a visual representation of the phase boundaries. The diagram helps in understanding the thermodynamic behavior of the cycle and identifying the efficiency improvements.

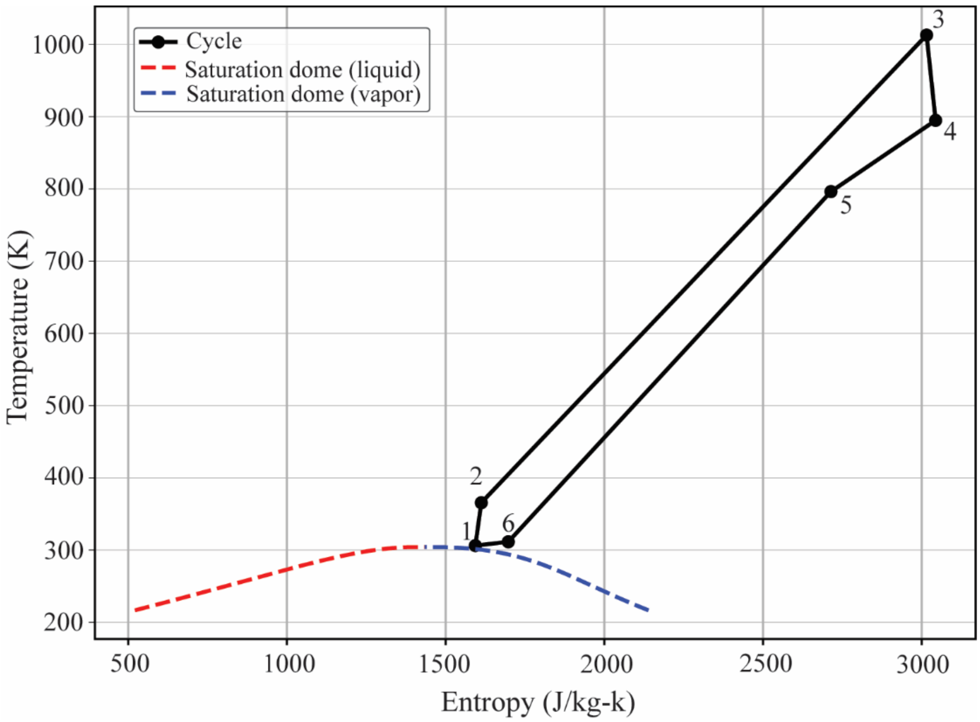

Fig. 4. Temperature-entropy diagram cascading nuclear cogeneration with sCO_2 cycle.

4. Thermodynamic Modelling

The thermodynamic cycle modeled in this study consists of several components including a reactor, compressor, turbocirculator, reboiler, heat exchanger, economizer, and recuperator. The modeling involves calculating the enthalpy, temperature, and entropy at various state points within the cycle. The calculations use the CoolProp library to determine the thermodynamic properties of the working fluids (CO_2 and He). Below is a detailed description of the mathematical modeling for each component in the cycle.

4.1 Reactor

The reactor provides thermal power to the cycle. The enthalpy change across the reactor is given by:

$$Q_{Re} = m_{Re} * \left(h_{i,_{Re}} - h_{o,_{Re}}\right) \tag{1}$$

The mass flow rate of helium in the reactor is calculated using the given thermal power and the enthalpy change:

$$m_{Re} = \frac{Q_{Re}}{h_{i,Re} - h_{o,Re}} \tag{2}$$

4.2 Compressor

The compressor increases the pressure of the CO_2. The isentropic efficiency of the compressor is used to determine the actual enthalpy at the outlet:

$$h_{o,Comp} = h_{i,Comp} + \frac{h_{o,Comp,is} - h_{i,Comp}}{\eta_{Comp}} \tag{3}$$

The isentropic outlet enthalpy of compressor is determined using the inlet entropy and the outlet pressure of compressor :

$$h_{o,Comp,is} = f\left(T_{o,Comp,is}, s_{i,Comp}, P_{o,Comp}\right) \tag{4}$$

The actual outlet temperature and entropy are then calculated using:

$$T_{o,Comp} = f\left(h_{o,Comp}, P_{o,Comp}\right) \tag{5}$$

$$s_{o,Comp} = f\left(T_{o,Comp}, P_{o,Comp}\right) \tag{6}$$

4.3 Turbocirculator

The turbocirculator operates similarly to the compressor but in the opposite direction, where it expands the working fluid:

$$h_{o,TC} = h_{i,TC} + \frac{h_{o,TC,is} - h_{i,TC}}{\eta_{TC}} \tag{7}$$

The isentropic outlet enthalpy of turbocirculator is determined using the inlet entropy and the outlet pressure of turbocirculator:

$$h_{o,TC} = f\left(T_{o,TC}, s_{i,TC}, P_{o_{TC}}\right) \tag{8}$$

The actual outlet temperature and entropy are then calculated using:

$$T_{o,TC} = f\left(h_{o,TC}, P_{o,TC}\right) \tag{9}$$

$$s_{o,TC} = f\left(T_{o,TC}, P_{o,TC}\right) \tag{10}$$

4.4 Reboiler

The reboiler heats the working fluid by condensing steam. The thermal power supplied by the reboiler is:

$$Q_{Reb} = \; m_{Reb} * \left(h_{o,Reb} - h_{i,Reb}\right) \tag{11}$$

4.5 Heat exchanger

The heat exchanger transfers thermal energy from the reactor to the working fluid. The enthalpy change across the heater is given by:

$$h_{o,Heater} = h_{i,heater} + \frac{\mathrm{Q}_{Heater}}{\mathrm{m}_{CO_2,Heater}} \tag{12}$$

The outlet temperature and entropy are then calculated using:

$$T_{o,Heater} = f\left(h_{o,Heater}, P_{o,Heater}\right) \tag{13}$$

$$s_{o,Heater} = f\left(T_{o,Heater}, P_{o,Heater}\right) \tag{14}$$

4.6 Economizer

The economizer preheats the working fluid using heat from the turbine exhaust. The enthalpy change across the economizer is given by:

$$h_{o,Eco} = h_{i,Eco} + \frac{\mathrm{Q}_{Eco}}{\mathrm{m}_{CO_2,Eco}} \tag{15}$$

The outlet temperature and entropy are then calculated using:

$$T_{o,Eco} = f\left(h_{o,Eco}, P_{o,Eco}\right) \tag{16}$$

$$s_{o,Eco} = f\left(T_{o,Eco}, P_{o,Eco}\right) \tag{17}$$

4.7 Recuperator

The recuperator improves cycle efficiency by recovering waste heat from the turbine exhaust and uses it to preheat the working fluid before it enters the heat exchanger. The enthalpy change across the recuperator is given by:

$$h_{o,Rec,hot} = h_{i,Rec,hot} - \eta_{Rec} * \left(h_{i,Rec,hot} - h_{o,Rec,is}\right) \tag{18}$$

$$h_{o,Rec,cold} = h_{i,Rec,cold} + \eta_{Rec} * \left(h_{i,Rec,hot} - h_{o,Rec,is}\right) \tag{19}$$

The overall cycle efficiency and net power output are calculated as:

$$\eta_{cycle} = \frac{W_{net}}{Q_{Reactor}} \tag{20}$$

$$W_{net} = W_{Turbine} - W_{Comp} \tag{21}$$

The thermodynamic properties at various state points in the cycle are calculated using the CoolProp library. The properties include enthalpy (h), temperature (T), and entropy (s). The library functions are used to compute these properties based on the state variables (pressure and temperature or enthalpy and pressure).

5. Results and Discussion

This study examines the performance of a nuclear cogeneration system integrated with a sCO_2 Brayton cycle, with a reboiler attached to provide useful heat/ processed steam for industrial applications. The system operates using heat from a nuclear reactor and utilizes two different working fluids: helium in the nuclear cycle and sCO_2 in the secondary cycle.

The performance of various parameters, such as the effect of turbine and compressor efficiency on the thermal efficiency of the cycle, was evaluated. Additionally, turbine power, power cycle efficiency, and net power were analyzed based on turbine inlet temperature and compressor pressure ratio.

5.1 Effect of turbine efficiency and compressor efficiency on thermal efficiency of the cycle

The relationship between turbine efficiency and the thermal efficiency of the cycle is illustrated in Fig. 5(a). As depicted in the plot, there is a clear linear relationship between turbine efficiency and the thermal efficiency of the cycle. Specifically, an increase in turbine efficiency from 0.50 to 1.0 results in a significant increase in the thermal efficiency of the cycle from approximately 0.25 to 0.45. This demonstrates that improving turbine efficiency can substantially enhance the overall thermal performance of the cycle.

The data points follow a nearly perfect linear tread, indicating that the thermal efficiency of the cycle is highly sensitive to change with turbine efficiency. This underscores the importance of optimizing turbine efficiency in efforts to maximize the thermal efficiency of the cycle.

Fig. 5(b) shows the effect of compressor efficiency on the thermal efficiency of the cycle. Similar to the turbine efficiency, there is a positive correlation between compressor efficiency and thermal efficiency. The plot reveals that as the compressor efficiency increases from 0.70 to 1.00, the thermal efficiency of the cycle increases from approximately 0.21 to 0.25.

Although the increase in thermal efficiency due to improved compressor efficiency is less steep compared to that observed with turbine efficiency, the trend is still positive and significant. This suggests that while optimizing compressor efficiency can contribute to enhanced thermal efficiency, its impact is slightly less pronounced than that of turbine efficiency.

The results from the plots indicate that both turbine and compressor efficiencies play critical roles in determining the thermal efficiency of the cycle. The linear relationship observed between turbine efficiency and thermal efficiency suggests that any improvements in turbine performance can lead to proportional gains in the cycle's thermal efficiency. On the other hand, the impact of compressor efficiency, while still positive, appears to be less substantial in comparison.

These findings highlight the importance of focusing on turbine efficiency as a primary target for improving the overall thermal efficiency of the cycle. However, improvements in compressor efficiency should not be neglected as they also contribute to the overall performance enhancement.

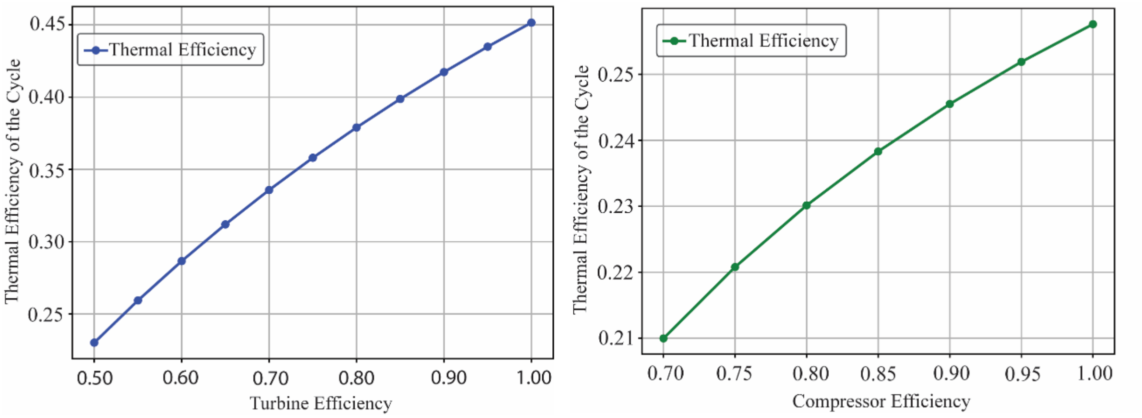

(a) *(b)*

Fig. 5. Effect of turbine and compressor efficiency on thermal efficiency of the cycle.

5.2 Variation in reboiler CO_2 inlet temperature and turbine power with respect to turbine inlet temperature and compressor pressure ratio

The results below investigate how turbine power output varies with reboiler CO_2 inlet temperature, turbine inlet temperature, and compressor pressure ratio. By analyzing these results, significant trends in turbine power generation are identified.

Fig. 6(a) examines the variation of turbine power with turbine inlet temperature and reboiler CO_2 inlet temperature. Increasing the turbine inlet temperature from 550°C to 725°C results in higher turbine power output across all examined reboiler CO_2 inlet temperatures, enhancing thermal efficiency. The reboiler CO_2 inlet temperature similarly boosts turbine power, with a more pronounced effect at higher turbine inlet temperatures. The maximum turbine power output, approximately 2.85 MW, is achieved at the highest turbine inlet temperature around 725°C and reboiler CO_2 inlet temperature around 740°C, while the minimum power output, around 1.41 MW, is observed at the lowest turbine inlet temperature i.e. 550°C and reboiler CO_2 inlet temperature at 580°C.

Fig. 6(b) illustrates the variation of turbine power as a function of compressor pressure ratio and reboiler CO_2 inlet temperature. As the compressor pressure ratio increases from 2.0 to 4.0, turbine power output consistently rises, indicating a positive correlation. Similarly, increasing the reboiler CO_2 inlet temperature from 580°C to 740°C significantly enhances turbine power output due to higher thermal efficiency. The combined effect of these variables shows that the highest turbine power output, approximately 3.35 MW, is achieved at the upper limits of both compressor pressure ratio around 4.0 and reboiler CO_2 inlet temperature around 740°C. Conversely, the lowest power output, around 1.35 MW, is observed at the lowest compressor pressure ratio of 2.0 and reboiler CO_2 inlet temperature at 580°C.

The analysis reveals that both turbine inlet temperature and compressor pressure ratio play crucial roles in determining turbine power output. Optimal performance is achieved at higher values of these parameters, along with higher reboiler CO_2 inlet temperatures. These results provide valuable insights for the design and operation of thermal power plants, aiming to improve efficiency and power generation capabilities.

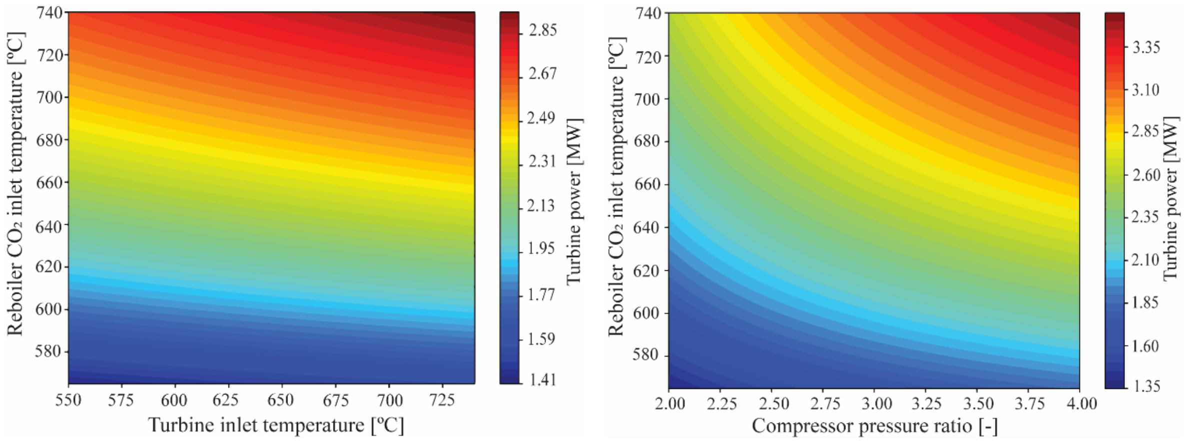

(a) *(b)*

Fig. 6. Variation in reboiler CO_2 inlet temperature and turbine power with respect to turbine inlet temperature and compressor pressure ratio.

5.3 Variation in reboiler CO_2 inlet temperature and power cycle efficiency with respect to turbine inlet temperature and compressor pressure ratio

The results presented below investigate the influence of reboiler CO_2 inlet temperature on power cycle efficiency, with a particular focus on variations in turbine inlet temperature and compressor pressure ratio. By analyzing two contour plots, we aim to provide insights for optimizing thermodynamic cycles for better performance.

Fig. 7(a) explores the impact of varying the turbine inlet temperature between 550°C to 740°C on power cycle efficiency while also varying the reboiler CO_2 inlet temperature. The lower turbine inlet temperatures from 550°C-600°C are associated with lower power cycle efficiency. Efficiency improves significantly as the turbine inlet temperature increases to around 675°C, beyond which further improvements are marginal.

Across different turbine inlet temperatures, the correlation between higher reboiler CO_2 inlet temperatures and improved efficiency remains consistent. However, the relative efficiency gain decreases as both the reboiler CO_2 inlet temperature and turbine inlet temperature increase, indicating a saturation effect at high temperatures.

Fig. 7(b) illustrates the relationship between power cycle efficiency, compressor pressure ratio ranging from 2.0 to 4.0, and reboiler CO_2 inlet temperature ranging between 580°C to 740°C. At lower compressor pressure ratios from 2.0 to 2.25, efficiency improves significantly with increasing reboiler CO_2 inlet temperature. However, beyond a compressor pressure ratio of 2.5, the efficiency gains plateau, and minimal changes are observed between pressure ratios of 3.5 and 4.0. This suggests that increasing the compressor pressure ratio beyond a certain threshold results in diminishing returns in terms of efficiency improvement.

The data also shows a marked increase in efficiency with rising reboiler CO_2 inlet temperature, particularly between 580°C and 700°C. Beyond 700°C, the efficiency gains taper off, indicating an optimal temperature range for maximizing efficiency.

These findings highlight the interactions between these operating parameters in the thermal power cycle, providing a framework for designing more efficient systems.

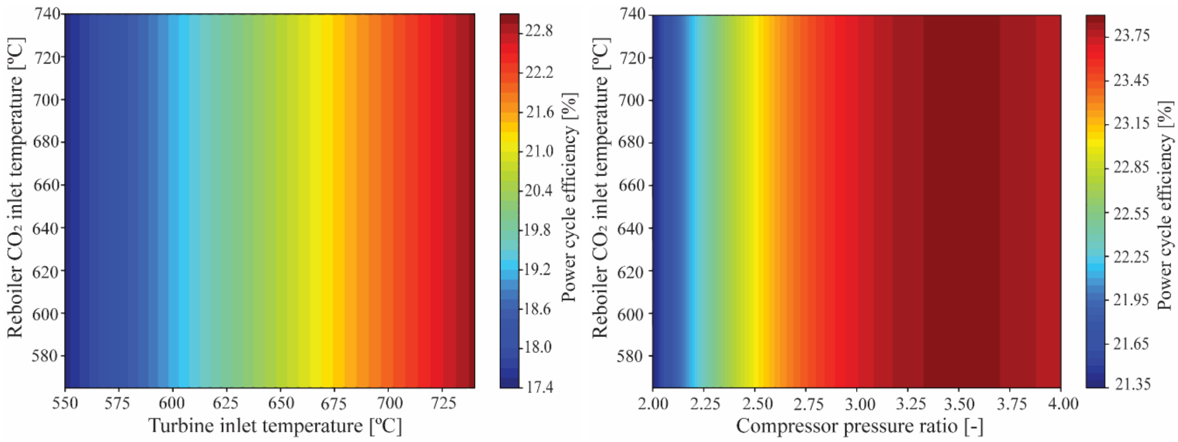

(a) *(b)*

Fig. 7. Variation in reboiler CO_2 inlet temperature and power cycle efficiency with respect to turbine inlet temperature and compressor pressure ratio.

5.4 Variation in reboiler CO_2 inlet temperature and net power with respect to turbine inlet temperature and compressor pressure ratio

The results below show the impact of reboiler CO_2 inlet temperature on net power output in a power generation system. The analysis focuses on the variations in net power concerning two key parameters turbine inlet temperature and compressor pressure ratio.

Fig. 8(a) illustrates the net power variation with turbine inlet temperature and reboiler CO_2 inlet temperature. The net power output increases almost linearly with rising turbine inlet temperatures from 550°C to 725°C, indicating the strong influence of turbine inlet temperature on overall power generation efficiency. At lower turbine inlet temperatures, the net power increases moderately with higher reboiler CO_2 inlet temperatures. However, at higher turbine inlet temperatures, the net power reaches higher values, showing that high turbine inlet temperatures significantly boost net power output. The optimal performance zones are identified at high turbine inlet temperatures between 700°C - 740°C and high reboiler CO_2 inlet temperatures from 680°C – 740 °C, where net power output peaks.

Fig. 8(b) shows the variation of net power output as a function of compressor pressure ratio and reboiler CO_2 inlet temperature. At lower reboiler CO_2 inlet temperatures from 580°C - 620°C, the net power shows high sensitivity to changes in the compressor pressure ratio. An increase in the pressure ratio from 2.0 to 4.0 leads to a significant rise in net power output. However, as the reboiler CO_2 inlet temperature increases from 620°C - 740°C, the sensitivity of net power to compressor pressure ratio diminishes, and the net power curve flattens, indicating diminishing returns with increasing pressure ratio. The net power is maximized at higher pressure ratios, particularly between 3.0 and 4.0, across most reboiler CO_2 inlet temperatures.

The analysis reveals that both compressor pressure ratio and turbine inlet temperature critically affect net power output in power cycles. The compressor pressure ratio's effect on net power diminishes as reboiler CO_2 inlet temperatures increase, whereas turbine inlet temperature consistently enhances net power output. These insights are vital for optimizing thermal systems, suggesting that maintaining high turbine inlet temperatures and selecting an appropriate compressor pressure ratio are key strategies for maximizing net power.

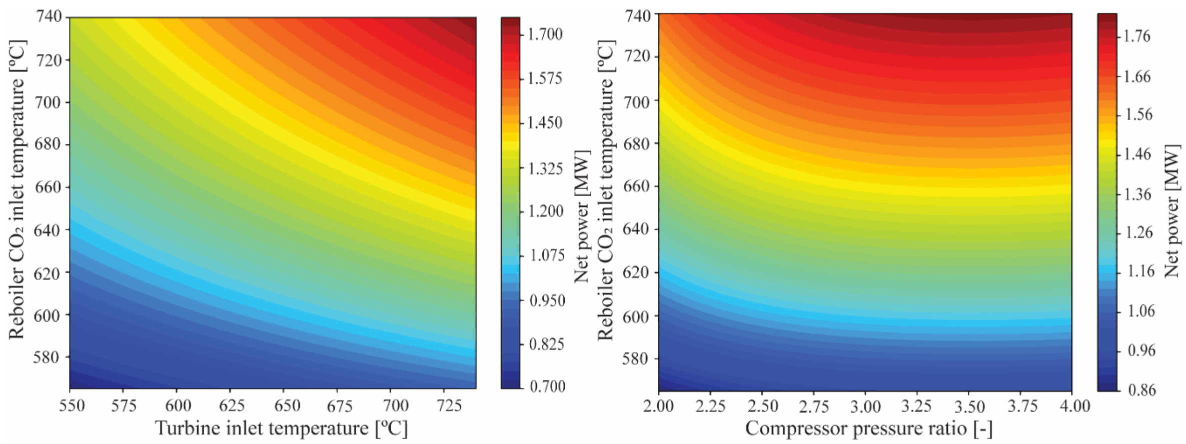

(a) *(b)*

Fig. 8. Variation in reboiler CO_2 inlet temperature and Net power with respect to turbine inlet temperature and compressor pressure ratio.

6. Conclusion

The integration of a reboiler into a nuclear-driven sCO_2 Brayton cycle has been demonstrated to significantly enhance power cycle efficiency and meet the heat demand for industrial processes. Through extensive thermodynamic analysis, this study explored the effects of turbine and compressor efficiencies on the thermal performance of the cycle, focusing on the variations in reboiler CO_2 inlet temperature, turbine power, power cycle efficiency, and net power with respect to turbine inlet temperature and compressor pressure ratio.

The findings indicate that optimal power cycle efficiency is achieved at higher reboiler CO_2 inlet temperatures, with substantial efficiency gains observed up to a certain threshold. Beyond this threshold, the efficiency improvements diminish. This balance between reboiler CO_2 inlet temperature, turbine inlet temperature, and compressor pressure ratio is critical for optimizing the system's performance.

This research also contributes to the efficient design and operation of thermal power plants by identifying optimal operational parameters that maximize net power output. Future work could focus on incorporating these findings into dynamic models for real-time optimization and control of power generation systems.

Additionally, future research could delve deeper into the combined optimization of turbine and compressor efficiencies, investigating potential nonlinearities and interactions. Additionally, understanding the mechanisms that influence these efficiencies could lead to more effective strategies for enhancing the overall thermal efficiency of nuclear-driven sCO_2 Brayton cycles. This research provides a valuable framework for designing more efficient thermal power systems, aligning with the goals of projects like "NC2I-R" and "Gemini+" for practical deployment in industrial applications.

Declaration of Competing Interest

The authors declare that they have no known competing financial interests or personal relationships that could have appeared to influence the work reported in this paper.

Abbreviations

CO_2	Cabon dioxide
h	enthalpy
He	Helium
HTGR	High temperature Gas-cooled reactor
m	mass flow rate
P	Pressure
Q	Thermal Power
s	entropy
sCO_2	supercritical carbon dioxide
SMR	Small modular reactor
T	Temperature
W	Work done

Subscripts

$comp$	compressor
Eco	Economizer
i	inlet
is	isentropic
o	outlet
Re	Reactor
Reb	Reboiler
Rec	Recuperator
TC	Turbocirculator

References

[1] K. Calvin, D. Dasgupta, G. Krinner, A. Mukherji, P.W. Thorne, C. Trisos, J. Romero, P. Aldunce, K. Barrett, G. Blanco, W.W.L. Cheung, S. Connors, F. Denton, A. Diongue-Niang, D. Dodman, M. Garschagen, O. Geden, B. Hayward, C. Jones, F. Jotzo, T. Krug, R. Lasco, Y.-Y. Lee, V. Masson-Delmotte, M. Meinshausen, K. Mintenbeck, A. Mokssit, F.E.L. Otto, M. Pathak, A. Pirani, E. Poloczanska, H.-O. Pörtner, A. Revi, D.C. Roberts, J. Roy, A.C. Ruane, J. Skea, P.R. Shukla, R. Slade, A. Slangen, Y. Sokona, A.A. Sörensson, M. Tignor, D. van Vuuren, Y.-M. Wei, H. Winkler, P. Zhai, Z. Zommers, J.-C. Hourcade, F.X. Johnson, S. Pachauri, N.P. Simpson, C. Singh, A. Thomas, E. Totin, A. Alegría, K. Armour, B. Bednar-Friedl, K. Blok, G. Cissé, F. Dentener, S. Eriksen, E. Fischer, G. Garner, C. Guivarch, M. Haasnoot, G. Hansen, M. Hauser, E. Hawkins, T. Hermans, R. Kopp, N. Leprince-Ringuet, J. Lewis, D. Ley, C. Ludden, L. Niamir, Z. Nicholls, S. Some, S. Szopa, B. Trewin, K.-I. van der Wijst, G. Winter, M. Witting, A. Birt, M. Ha, IPCC, 2023: Climate Change 2023: Synthesis Report. Contribution of Working Groups I, II and III to the Sixth Assessment Report of the Intergovernmental Panel on Climate Change [Core Writing Team, H. Lee and J. Romero (eds.)]. IPCC, Geneva, Switzerland., 2023. https://doi.org/10.59327/IPCC/AR6-9789291691647.

[2] B. Khan, M.H. Kim, Energy and Exergy Analyses of a Novel Combined Heat and Power System Operated by a Recuperative Organic Rankine Cycle Integrated with a Water Heating System, Energies (Basel) 15 (2022). https://doi.org/10.3390/en15186658.

[3] G. Li, G. Du, G. Liu, J. Yan, Study on the dynamic characteristics, control strategies and load variation rates of the concentrated solar power plant, Appl Energy 357 (2024). https://doi.org/10.1016/j.apenergy.2023.122538.

[4] J. Syblík, J. Štěpánek, L. Veselý, S. Entler, V. Dostál, Preliminary design of supercritical CO2 axial compressor for fusion and nuclear power plants, Fusion Engineering and Design 192 (2023). https://doi.org/10.1016/j.fusengdes.2023.113770.

[5] M. Biondi, A. Giovannelli, G. Di Lorenzo, C. Salvini, Techno-economic analysis of a sCO2 power plant for waste heat recovery in steel industry, Energy Reports 6 (2020) 298–304. https://doi.org/10.1016/j.egyr.2020.11.147.

[6] N.A. Mohammed Almefreji, B. Khan, M.-H. Kim, machines Thermodynamic Performance Analysis of Solar Based Organic Rankine Cycle Coupled with Thermal Storage for a Semi-Arid Climate, (2021). https://doi.org/10.3390/machines.

[7] Q. Zhao, J. Xu, M. Hou, D. Chong, J. Wang, W. Chen, Dynamic characteristic analysis of SCO2 Brayton cycle under different turbine back pressure modes, Energy 293 (2024). https://doi.org/10.1016/j.energy.2024.130563.

[8] J. Tang, Q. Zhang, Z. Zhang, Q. Li, C. Wu, X. Wang, Development and performance assessment of a novel combined power system integrating a supercritical carbon dioxide Brayton cycle with an absorption heat transformer, Energy Convers Manag 251 (2022). https://doi.org/10.1016/j.enconman.2021.114992.

[9] I. - International Energy Agency, World Energy Outlook 2023, 2023. www.iea.org/terms.

[10] G. Wrochna, M. Fütterer, D. Hittner, Nuclear cogeneration with high temperature reactors, EPJ Nuclear Sciences & Technologies 6 (2020) 31. https://doi.org/10.1051/epjn/2019023.

[11] IAEA., Industrial Applications of Nuclear Energy., IAEA, 2017.

[12] V. Dostal, P. Hejzlar, M.J. Driscoll, High-performance supercritical carbon dioxide cycle for next-generation nuclear reactors, Nucl Technol 154 (2006) 265–282. https://doi.org/10.13182/NT154-265.
[13] S. Yun, D. Zhang, X. Li, X. Zhou, D. Jiang, X. Lv, W. Wu, Z. Feng, X. Min, W. Tian, S. Qiu, G.H. Su, Design, optimization and thermodynamic analysis of SCO2 Brayton cycle system for FHR, Progress in Nuclear Energy 157 (2023). https://doi.org/10.1016/j.pnucene.2023.104593.
[14] IAEA Nuclear Energy Series @, n.d. http://www.iaea.org/Publications/index.html.
[15] Clean Growth - Transforming Heating - Overview of Current Evidence, 2018.
[16] M.A. Fütterer, R. Pabarcius, S. Hübner, L. Pieńkowski, W. Brudek, P. Darnowski, M. Pawluczyk, B. Chmielarz, M. Šilhan, Nuclear process heat application options: Highlights from the European GEMINI+ project, Nuclear Engineering and Design 396 (2022). https://doi.org/10.1016/j.nucengdes.2022.111879.
[17] D. Prochazkova, J. Prochazka, V. Dostal, Resiliency of Industrial Complexes Powered by Small Modular Reactors, in: Research Publishing Services, 2023: pp. 1506–1513. https://doi.org/10.3850/978-981-18-8071-1_p068-cd.
[18] V. Dostal, P. Hejzlar, M.J. Driscoll, The supercritical carbon dioxide power cycle: Comparison to other advanced power cycles, Nucl Technol 154 (2006) 283–301. https://doi.org/10.13182/NT06-A3734.
[19] N. Pardo, K. Vatopoulos, A. Krook-Riekkola, J.A. Moya, A. Perez, European Commission. Joint Research Centre. Institute for Energy and Transport., Heat and cooling demand and market perspective., Publications Office, 2012.
[20] M.A. Fütterer, R. Pabarcius, S. Hübner, L. Pieńkowski, W. Brudek, P. Darnowski, M. Pawluczyk, B. Chmielarz, M. Šilhan, Nuclear process heat application options: Highlights from the European GEMINI+ project, Nuclear Engineering and Design 396 (2022). https://doi.org/10.1016/j.nucengdes.2022.111879.
[21] V. Kindra, I. Maksimov, D. Patorkin, A. Rogalev, N. Rogalev, Thermodynamic Analysis and Optimization of Binary CO2-Organic Rankine Power Cycles for Small Modular Reactors, Energies 17 (2024). https://doi.org/10.3390/en17102377.